Experimental assessment of vertical spanning strengthened masonry infills under out-of-plane actions

Mariano Di Domenico[a], Paolo Ricci[a], Gerardo M. Verderame[a], Alberto Balsamo[a], Gennaro Maddaloni[a]
[a] *Dipartimento di Strutture per l'Ingegneria e l'Architettura, Università degli Studi di Napoli Federico II, Via Claudio 21, 80135 Naples, Italy*

Keywords: infill wall; out-of-plane; seismic; strengthening; repairment

ABSTRACT
Recent studies, as well as past earthquake experience, demonstrated that slender unreinforced masonry infills are significantly vulnerable with respect to out-of-plane actions. The out-of-plane collapse of infills significantly increases the repairment and refurbishment costs after earthquakes of reinforced concrete buildings and, above all, is highly detrimental for human life safety.
For this reason, the interest on the experimental and numerical studies dedicated to the assessment of the effectiveness of out-of-pane repairing, strengthening and reinforcement techniques of masonry infills is growing, especially in recent years.
In this work, experimental tests performed at the Department of Structures for Engineering and Architecture of University of Naples Federico II to characterize the out-of-plane response of one-way spanning unreinforced and reinforced masonry infills are presented. Namely, an out-of-plane test is performed on an "as-built" specimen, whose performance is compared with the experimental response of specimens strengthened by applying two different techniques, a fiber reinforced polymer and a fabric reinforced cementitious mortar. In addition, after test, the as-built specimen is repaired by applying the fiber reinforced polymer and tested again. The response of the repaired specimen is presented and discussed.

1 INTRODUCTION

In past and recent studies, it has been demonstrated that unreinforced masonry (URM) infill walls in Reinforced Concrete (RC) frames are prone to damage and, potentially, collapse due to out-of-plane (OOP) seismic actions (Calvi and Bolognini 2001, Guidi et al. 2013, Mosalam and Günay 2015, Furtado et al. 2016, Longo et al. 2018, Ricci et al. 2018a-b-c, Di Domenico et al. 2019). Unfortunately, the experimental and numerical outcomes presented in the literature in the last 30 years have been confirmed by the experience of past and recent earthquakes, during which OOP collapses of masonry enclosures have been registered.

For all these reasons, experimental and numerical research also investigated the effectiveness of strengthening and reinforcement techniques to improve the OOP seismic performance of masonry infills, in some cases also considering the effect of the in-plane (IP) damage on the OOP response of strengthened/reinforced masonry infills (IP/OOP interaction). More specifically, the efficiency of steel reinforcement (internal vertical and/or horizontal rebars or wire meshes plastered to the infill surface) was investigated, e.g., in (Dawe and Seah 1989, Angel et al. 1994, Calvi and Bolognini 2001, Pereira et al. 2011, Guidi et al. 2013, Lourenço et al. 2016). The effectiveness of Fiber Reinforced Polymers (FRP) was tested, e.g., in (Velazquez-Dimas and Ehsani 2000, Hrynyk and Myers 2008, Lunn and Rizkalla 2011, Valluzzi et al. 2014), while the OOP strengthening capacity of Fabric Reinforced Cementitious Matrices (FRCM) was assessed, e.g., in (da Porto et al. 2015, Ismail et al. 2018, Koutas and Bournas 2019). Modelling proposals for the evaluation of the OOP response and strength of reinforced/strengthened masonry infills were proposed in (Dawe and Seah 1989, Binici et al. 2007, Hrynyk and Myers 2008, Lunn and Rizkalla 2014, D'Antino et al. 2018).

In this work, the results of OOP experimental tests on unreinforced and strengthened masonry infills in RC frames are presented. The main aims of the experimental program are:

1. Investigating the strengthening effectiveness of two different techniques, a Glass FRCM (specimen OOP_2E_RG) and an FRP (specimen OOP_2E_EQ), by comparing the experimental response of two strengthened specimen with that exhibited by an as-built URM infill wall (specimen OOP_2E_AB);
2. Investigating the repairing effectiveness of the FRP, which was applied to the as-built specimen after the OOP test (specimen OOP_2E_RE);
3. Investigating the strength mechanism occurring in strengthened masonry infills under OOP actions, namely the potential occurrence of a flexural strength mechanism and of arching effect.

Principally to achieve the third aim by considering the simplest condition, all the specimens tested were mortared to the confining structural elements only along the upper and the lower edges. In other words, the infill walls tested were detached from the RC columns of the confining frame. In this way, only one-way vertical arching effect can occur in the unreinforced specimen (OOP_2E_AB), while in the strengthened specimens (OOP_2E_RG, OOP_2E_EQ, and OOP_2E_RE) only one-way flexural bending and/or one-way vertical arching are expected to occur.

2 SPECIMENS AND MATERIAL PROPERTIES

The RC frames tested were realized with class C32/40 concrete and reinforcement rebars with characteristic yielding strength equal to 450 N/mm^2. The frame was 2:3 scaled and was

designed according to the seismic provisions provided by the Italian building code NTC2008 (NTC2008 2008). Construction drawings of the RC frames are reproduced in Figure 1.

The experimental tests were performed on masonry infills realized with clay hollow units placed with horizontal holes and class M5 cementitious mortar. The clay hollow units used were 250 mm high, 250 mm wide and 80 thick. Infill walls were 1830 mm high, 2350 mm wide and 80 mm thick. The mechanical properties of masonry reported in Table 1 are referred to masonry wallets identical (for material, dimensions and workmanship) to those realized for the characterization of the specimens herein presented.

Specimen OOP_2E_AB was tested without any strengthening material.

Specimen OOP_2E_RG was strengthened by using a fiber-reinforced cementitious mortar (FRCM) with a bidirectional primed alkali-resistant fiberglass mesh with mesh size equal to 12.7 mm × 12.7 mm. More specifically, a 5 mm thick layer of plaster was applied on the infill surface; then, the fiberglass mesh was embedded in the plaster by covering it with a further 5 mm thick layer of plaster. The fiberglass mesh was not connected to the RC frame elements and was applied by using 0.45 m wide stripes with a 0.10 m overlap from stripe to stripe. The mechanical properties of both materials are reported in Table 1. Pictures taken during the application of the FRCM are reported in Figure 2.

Specimen OOP_2E_EQ was strengthened by using a bidirectional primed fiberglass fabric applied to the infill surface by using a water and polyurethane-based adhesive. The fiberglass fabric was not connected to the RC frame elements and was applied by using two 1.00 m wide stripes at the infill lateral edges together with a central 0.75 m wide stripe with a 0.20 m overlapping on both sides. The mechanical properties of the fiberglass fabric are reported in Table 1. Pictures taken during the application of the material are reported in Figure 3.

Specimen OOP_2E_RE was obtained by repairing specimen OOP_2E_AB after the OOP test. First, four upper clay units that crushed during test OOP_2E_AB were replaced by using identical clay units. In addition, cracks were filled by using the fibre reinforced mortar also used for specimen OOP_2E_RG, as shown in Figure 4. Finally, the fiberglass fabric used for specimen OOP_2E_EQ was applied to the infill surface.

In all cases, the strengthening materials were applied only on one side of the infill, i.e., on the surface expected as in tension (at least in the central part) given the monotonic loading direction.

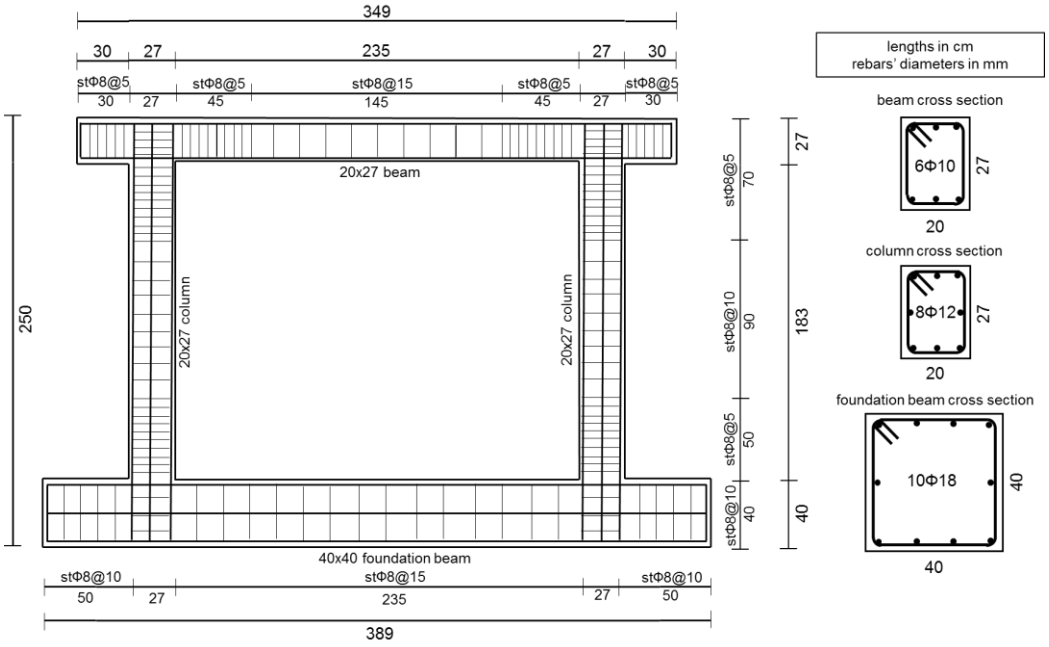

Figure 1. Construction drawing of the RC frame.

material	property	units	average value
concrete	mean compressive strength	[N/mm^2]	46.2
reinforcement steel	mean yielding stress	[N/mm^2]	497
masonry	vertical compressive strength	[N/mm^2]	1.81
masonry	vertical elastic modulus	[N/mm^2]	1090
masonry	crushing strain	[%]	0.17
fiber reinforced mortar	compressive strength	[N/mm^2]	37.6
fiber reinforced mortar	elastic modulus in compression	[N/mm^2]	10000*
fiber reinforced mortar	tensile strength (flexural)	[N/mm^2]	8.46
fiberglass mesh	weight	[g/m^2]	125*
fiberglass mesh	equivalent thickness of dry mesh	[mm]	0.024*
fiberglass mesh	tensile strength	[N/mm^2]	1276*
fiberglass mesh	elastic modulus	[N/mm^2]	72000*
fiberglass mesh	ultimate strain	[%]	1.8*
fiberglass fabric	weight	[g/m^2]	286*
fiberglass fabric	equivalent thickness of dry fabric	[mm]	0.057*
fiberglass fabric	tensile strength	[N/mm^2]	1620*
fiberglass fabric	elastic modulus	[N/mm^2]	42000*
fiberglass fabric	ultimate strain	[%]	4.0*

*: nominal value declared by the producer

Table 1. Materials' mechanical properties.

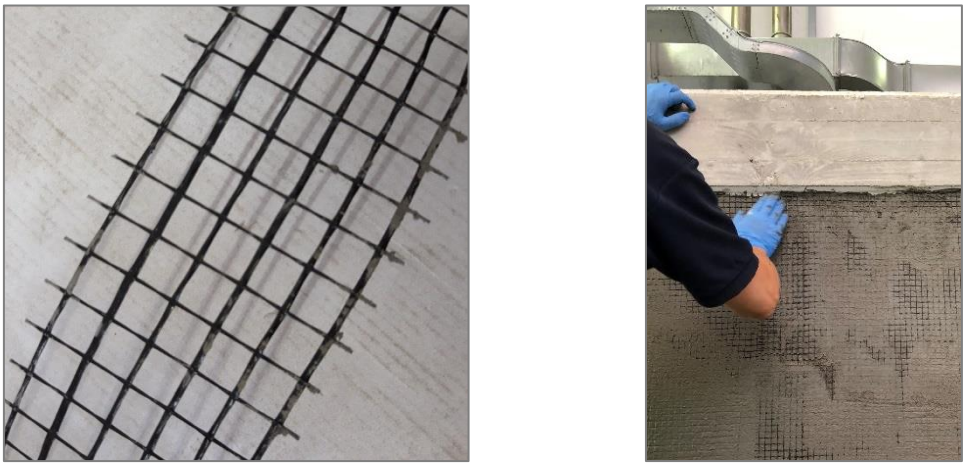

(a) (b)

Figure 2. Specimen OOP_2E_RG. (a) Fiberglass mesh; (b) embedment of the fiberglass mesh in the first layer of fiber-reinforced mortar.

(a) (b)

Figure 3. Specimen OOP_2E_EQ: (a) application of the adhesive; (b) application of the fabric.

The experimental tests were performed by applying the OOP load in displacement control on four loading points placed at roughly one-third of the infill height/width. Further details on the loading system and on the experimental setup can be found in (Di Domenico et al. 2018). The instrumentation layout consists in 5 laser displacement transducers and in 15 Linear Variable Displacement Transducer (LVDT), as shown in Figure 5. The vertical LVDT placed above the RC upper beam is used to measure the outward displacement of the central point of the RC frame upper beam. Such a vertical displacement is due, potentially, to the deflection of the RC frame upper beam due to vertical arching thrusts forming in the infill thickness if arching action occurs, as theorized by (Dawe and Seah 1989) and experimentally observed in (Verderame et al. 2019).

(a) (b)

Figure 4. Specimen OOP_2E_RE (a) after replacing damaged clay units and filling cracks and (b) after the application of the fiberglass fabric.

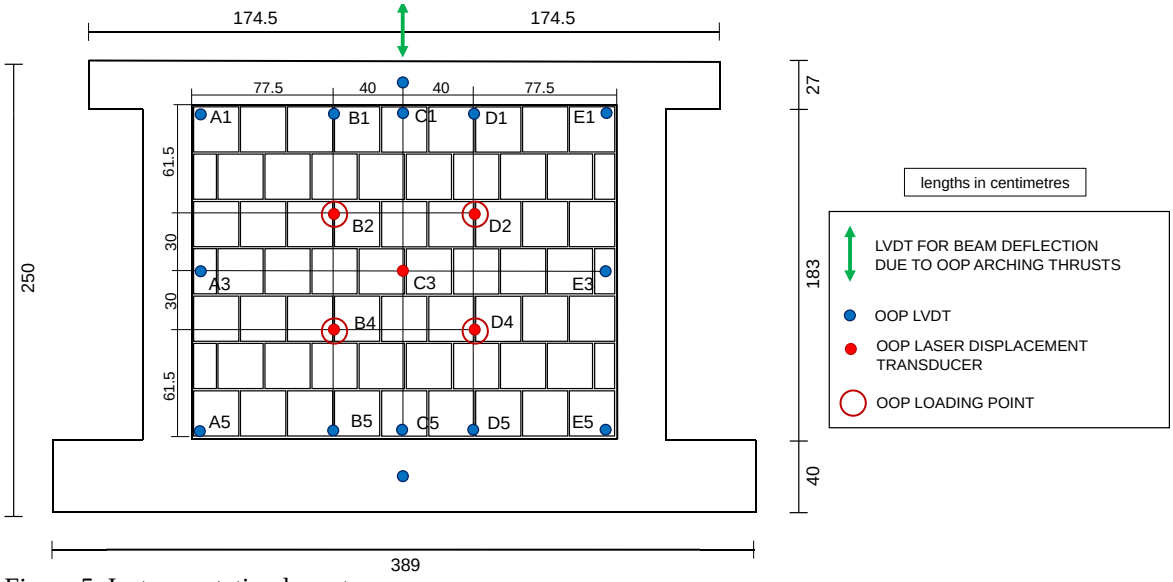

Figure 5. Instrumentation layout.

3 EXPERIMENTAL TESTS

3.1 Test OOP_2E_AB

The OOP force-displacement response of the as-built URM specimen OOP_2E_AB is reported in Figure 6a. The first visible horizontal crack appeared near the infill mid-height, on the right side, for an OOP force equal to 5.7 kN and for an OOP displacement equal to 2.1 mm. Up to this point, the maximum deflection registered for the upper beam was equal to 0.12 mm, most likely due to a (very small) torsional action transferred from the infill wall to the beam. However, after first cracking, a significant deflection of the upper beam begun, as shown by the abrupt reduction of the tangent stiffness in the OOP force – beam deflection reported in Figure 6b. This means that, after cracking, at a small increase of the external OOP force acting on the infill wall, a significant increase of the action applied to the RC frame upper beam occurred. In other words, arching thrusts formed in the infill thickness. These thrusts are transmitted to the RC upper beam, which, due to this action, deflects, as theorized also in (Dawe and Seah 1989). Hence, phase I in Figure 6a is characterized by a flexural strength mechanism of the infill wall panel, while phase II is characterized by the development of arching effect. A significant reduction of the infill OOP tangent stiffness was observed. Up to the attainment of the maximum load resistance, the first crack extended and covered the entire width of the infill. The maximum strength was equal to 9.9 kN and was registered for an OOP displacement equal to 13.9 mm. A steep softening branch was then registered, with a 20% strength degradation at an OOP displacement equal to 17.1

mm. During the last part of the test, the upper corners of the infill wall were crushing with detachment of bricks' exterior tiles. For this reason, phase III in Figure 6a is characterized by the collapse of arching action due to masonry crushing. A picture of the specimen at the end of test is reported in Figure 7.

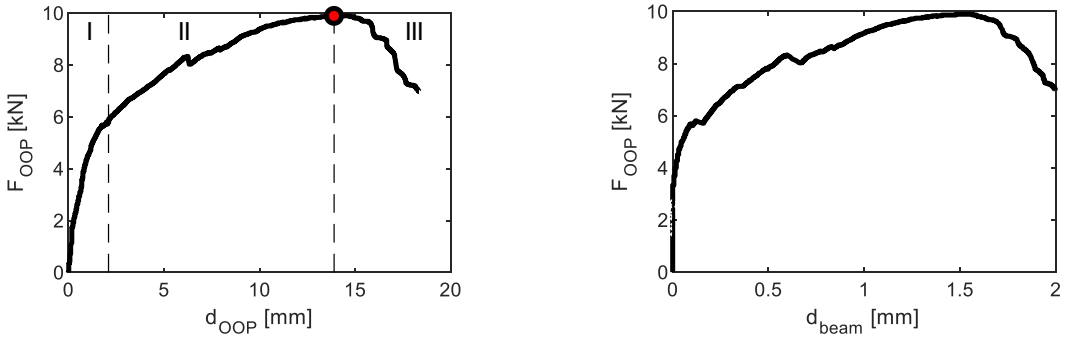

(a) (b)

Figure 6. Force-displacement response of specimen OOP_2E_AB: (a) OOP force-displacement, (b) OOP force-beam deflection.

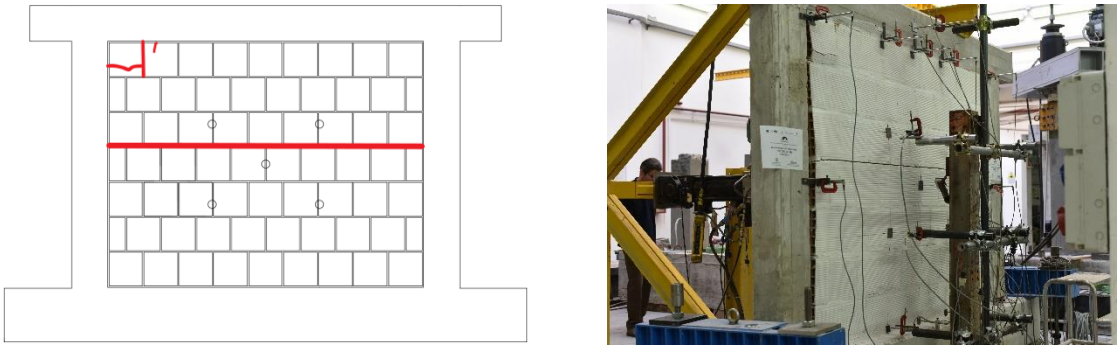

(a) (b)

Figure 7. Specimen OOP_2E_AB at the end of the test: (a) cracking pattern, (b) photograph.

3.2 Test OOP_2E_RG

The OOP force-displacement response of the specimen strengthened with mortar and fiberglass mesh, OOP_2E_RG, is reported in Figure 8a. The first visible horizontal crack appeared in the upper part of the infill, for an OOP force equal to 20.3 kN and for an OOP displacement equal to 2.8 mm. At this point, the deflection of the upper beam, revealing the occurrence of arching action, begun, as shown in Figure 8b. Hence, phase I in Figure 8a is characterized by a flexural strength mechanism of the infill wall panel, while phase II is characterized by the development of arching effect. A drop in the load bearing capacity was observed up to a load equal to 17.0 kN registered for an OOP displacement equal to 3.6 mm. Then, the OOP load increased with a significant reduction of the tangent stiffness. Up to the attainment of the maximum load resistance, the first crack extended and covered the entire width of the infill. The maximum strength was equal to 28.4 kN and was registered for an OOP displacement equal to 11.0 mm. A very steep softening branch was then registered, with a 20% strength degradation at an OOP displacement equal to 13.0 mm. During this phase, hairline horizontal cracks appear along the entire width of the infill, in its upper part. The test ended at an OOP force equal to 0.6 kN and at an OOP displacement equal to 16.1 mm. During the last part of the test, a wide horizontal crack appeared at the interface between the infill wall and the RC upper beam with to masonry crushing in correspondence with the upper row of clay units. This occurred despite the maximum compression is expected in the central zone of the infill. For this reason, phase III in Figure 8a is characterized by the collapse of arching action due to masonry crushing, as also demonstrated by the unloading of the RC upper beam shown in Figure 8b. A picture of the specimen at the end of test is reported in Figure 9. It should be noted that no damage was detected for the fiberglass mesh at the end of the test.

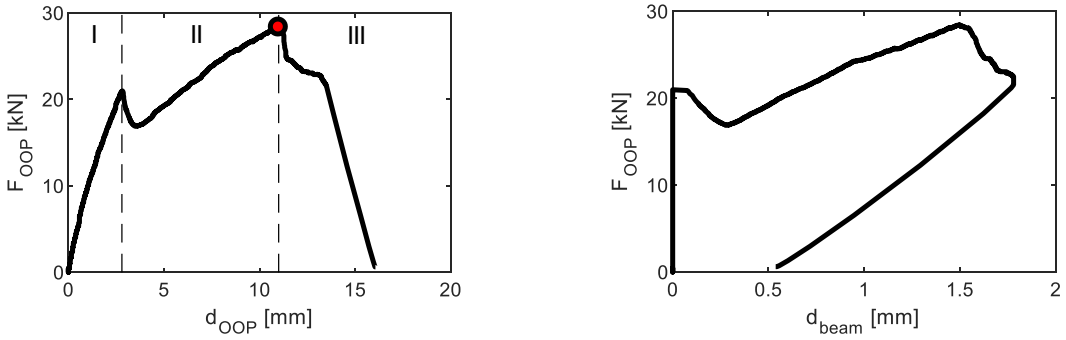

(a) (b)

Figure 8. Force-displacement response of specimen OOP_2E_RG: (a) OOP force-displacement, (b) OOP force-beam deflection.

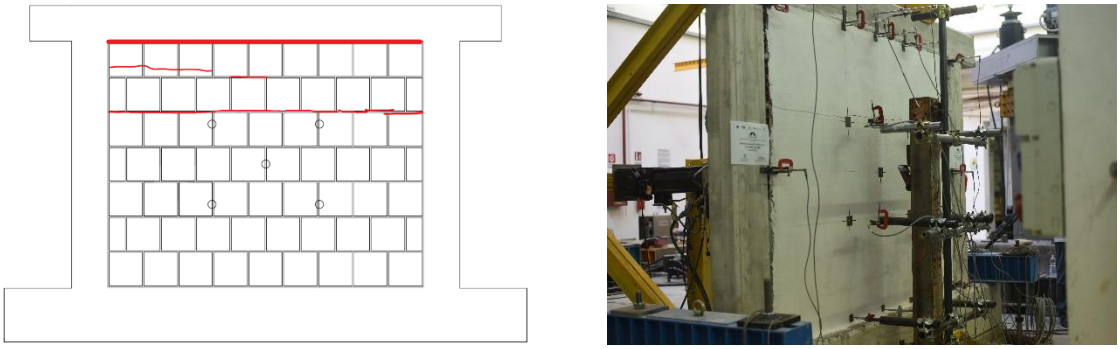

(a) (b)

Figure 9. Specimen OOP_2E_RG at the end of the test: (a) cracking pattern, (b) photograph.

3.3 Test OOP_2E_EQ

The OOP force-displacement response of the specimen strengthened with the fiberglass fabric, OOP_2E_EQ, is reported in Figure 10a. In this case, cracks in the infill during the test are not immediately visible, as the strengthening fabric cover them up. The first noticeable nonlinearity in the force-displacement graph, at which a significant reduction of the infill OOP tangent stiffness was observed, occurred for an OOP force equal to 8.2 kN and for an OOP displacement equal to 1.7 mm. Phase I in Figure 10a is characterized by a flexural strength mechanism of the infill wall panel: in fact, at this point, the deflection of the upper beam, revealing the occurrence of arching action, begun, as shown in Figure 10b. The maximum strength was equal to 19.1 kN and was registered for an OOP displacement equal to 9.7 mm. So, phase II in Figure 10a is characterized by the development of arching effect. A very steep softening branch was then registered, with a 20% strength degradation at an OOP displacement equal to 10.1 mm. During this phase, hairline horizontal cracks appear along the entire width of the infill, in its upper part. The test ended at an OOP force equal to 5.6 kN and at an OOP displacement equal to 11.8 mm. During the very last part of the test, a wide horizontal crack appeared in the lower part of the infill, presumably due to masonry crushing, even though the maximum compression is expected in the central part of the infill wall. Phase III in Figure 10a is characterized by the collapse of arching action, as also demonstrated by the unloading of the RC upper beam shown in Figure 10b. A picture of the specimen at the end of test is reported in Figure 11. It should be noted that no damage was detected for the fiberglass fabric at the end of the test, even if it resulted locally detached from the infill surface due to, most likely, debonding phenomena.

3.4 Test OOP_2E_RE

The OOP force-displacement response of the specimen repaired with the fiberglass fabric, OOP_2E_RE, is reported in Figure 12a. Also in this case, cracks in the infill during the test are not immediately visible, as the fiberglass fabric cover them up. The first noticeable nonlinearity in the force-displacement graph, at which a significant reduction of the infill OOP tangent stiffness was observed, occurred for an OOP force equal to 8.1 kN and for an OOP displacement equal to 2.1 mm. Phase I in Figure 12a is characterized by a flexural strength mechanism of the infill wall panel. In fact, at this point, the deflection of the upper beam, revealing the occurrence of arching action, begun, as shown in Figure 12b. The maximum strength was equal to 16.3 kN and was registered for an

OOP displacement equal to 12.1 mm. Phase II in Figure 12a is characterized by the development of arching effect. At the attainment of peak load, a horizontal crack opened at one upper corner. A very steep softening branch was then registered, with a 20% strength degradation at an OOP displacement equal to 13.0 mm. The test ended at an OOP force equal to 5.2 kN and at an OOP displacement equal to 14.2 mm. During the last part of the test, a wide horizontal crack appeared in the lower part of the infill, similarly to specimen OOP_2E_EQ. Phase III in Figure 12a is characterized by the collapse of arching action, as also demonstrated by the unloading of the RC upper beam shown in Figure 12b. A picture of the specimen at the end of test is reported in Figure 13. Also in this case, no damage was detected for the fiberglass fabric at the end of the test, even if it resulted locally detached from the infill surface due to, most likely, debonding phenomena.

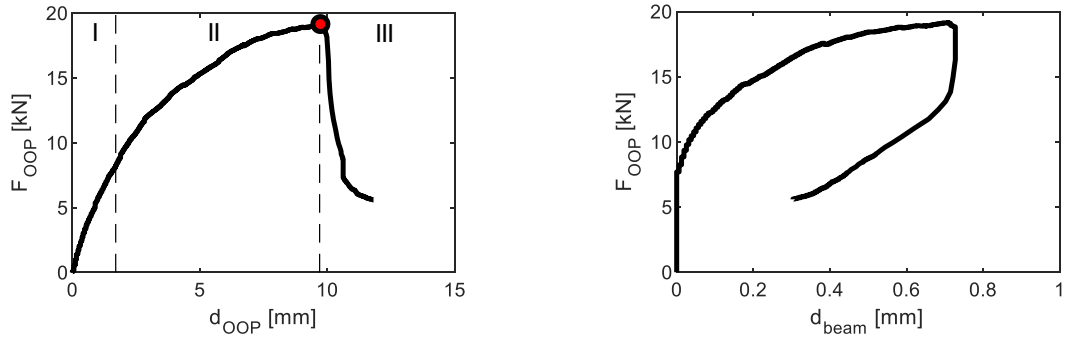

(a) (b)

Figure 10. Force-displacement response of specimen OOP_2E_EQ: (a) OOP force-displacement, (b) OOP force-beam deflection.

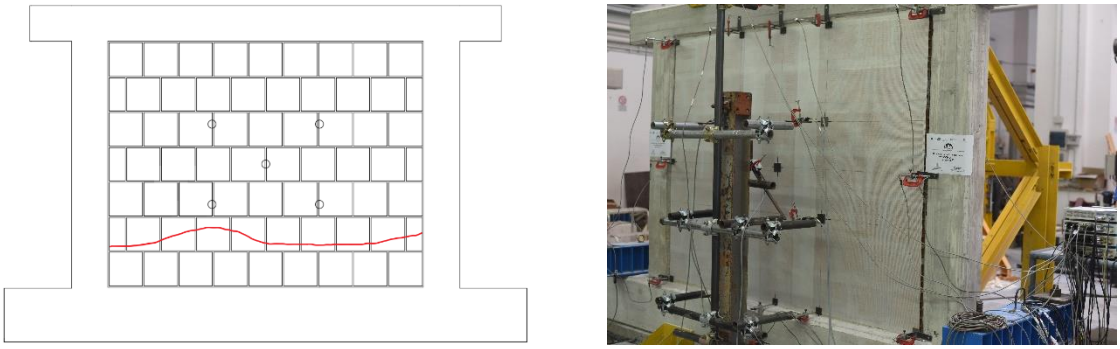

(a) (b)

Figure 11. Specimen OOP_2E_EQ at the end of the test: (a) cracking pattern, (b) photograph.

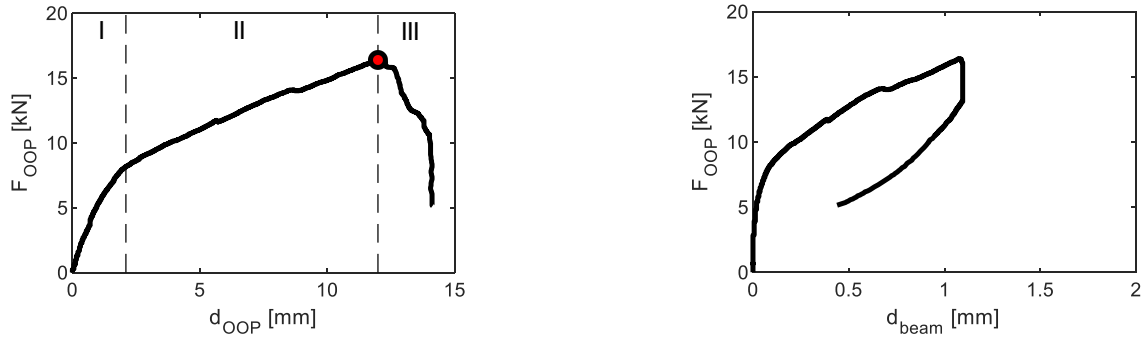

(a) (b)

Figure 12. Force-displacement response of specimen OOP_RE_EQ: (a) OOP force-displacement, (b) OOP force-beam deflection.

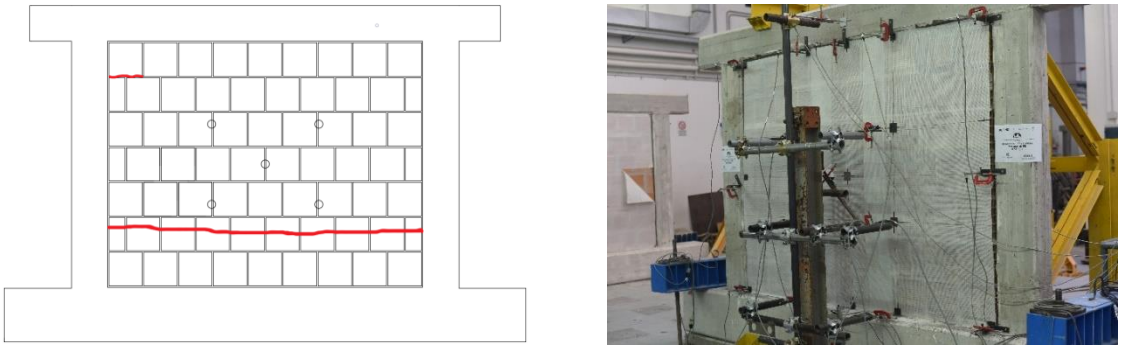

(a) (b)

Figure 13. Specimen OOP_2E_RE at the end of the test: (a) cracking pattern, (b) photograph.

4 PRELIMINARY DISUSSION OF THE EXPERIMENTAL RESULTS

The OOP response of specimens AB, RG and EQ is compared in Figure 14 and in Table 2. The ultimate displacement reported in Table 2 is conventionally defined as the OOP central displacement at an OOP strength degradation equal to 20%.

It is observed that the strength of specimen OOP_2E_RG is nearly three times the strength of the as-built specimen (+187%), while the strength of specimen OOP_2E_EQ is nearly two times the strength of the as-built infill (+93%). However, there is no improvement of the ductility capacity (i.e., the ratio of the conventional ultimate displacement over the displacement at peak load resistance) of the infill wall. In other words, the strengthening techniques tested are effective in increasing the OOP strength of infills while they do not influence their ductility capacity.

As expected, the OOP load carried by the strengthened infills by a pure flexural strength mechanism, i.e., the load at which arching action forms, is higher than that carried by the URM specimen. Namely, the OOP load at the occurrence of arching action is equal to 5.7 kN for specimen OOP_2E_AB, to 20.3 kN (+256%) for specimen OOP_2E_RG, to 8.2 kN (+44%) for specimen OOP_2E_EQ (see Figure 14b). The increase for specimen OOP_2E_RG is due to two factors: on one hand, the increment of the infill thickness due to the fiber mortar layer applied; on the other hand, the high tensile strength of the fiber reinforced mortar used. The increase for specimen OOP_2E_EQ is due, most likely, to the fact that a certain part of tensile stresses induced by the external load are transmitted to the FRP layer.

As shown in Figure 15, the initial stiffness of the specimens is quite identical for specimens OOP_2E_AB, OOP_2E_EQ and OOP_2E_RE, as expected, as in this case the strengthening fabric has a negligible thickness with respect to the masonry infill; on the contrary, a greater initial stiffness is observed for specimen OOP_2E_RG, in which the strengthening plaster layer is 10 mm thick. It is shown, in addition, that the experimental initial stiffness of specimens OOP_2E_AB, OOP_2E_EQ and OOP_2E_RE is consistent with the elastic stiffness of a beam clamped at both edges.

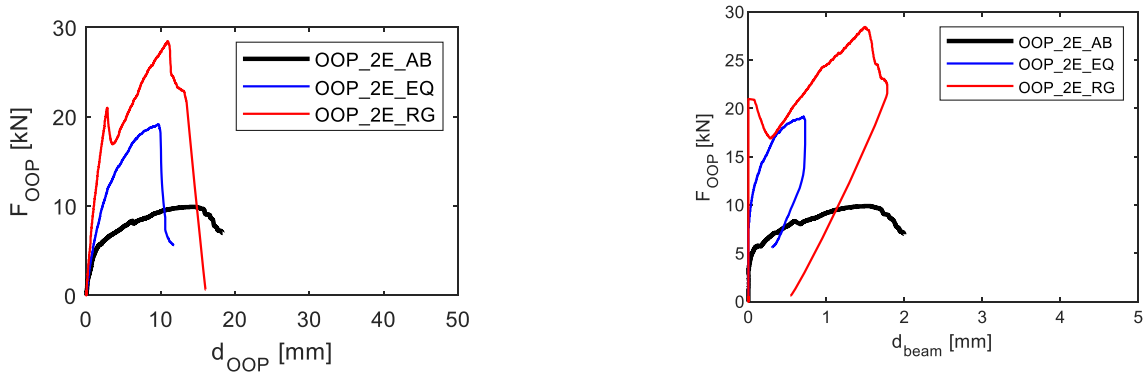

(a) (b)

Figure 14. Comparison of the responses of specimens: (a) OOP force-displacement, (b) OOP force-beam deflection.

specimen	strength [kN]	displacement at peak load [mm]	ultimate displacement [mm]	ductility
OOP_2E_AB	9.9	13.9	17.1	1.23
OOP_2E_RG	28.4 (+187%)	11.0	13.0	1.18
OOP_2E_EQ	19.1 (+93%)	9.7	10.1	1.04

Table 2. Comparison of significant tests' results for specimens OOP_2E_AB, OOP_2E_RG, OOP_2E_EQ.

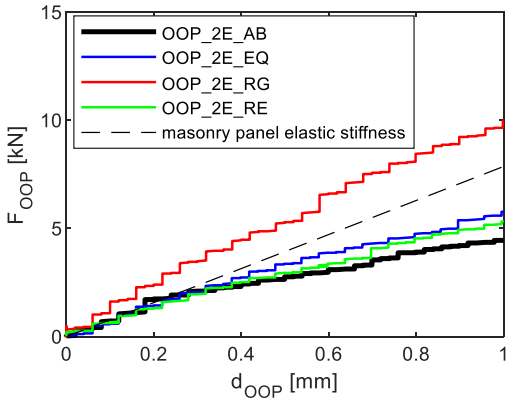

Figure 15. Comparison of the initial force-displacement responses of specimens.

The OOP response of specimens OOP_2E_AB, OOP_2E_EQ and of the repaired specimen OOP_2E_RE is compared in Figure 16 and in Table 3.

As should be expected, the specimen repaired with the fiberglass fabric exhibited an intermediate strength with respect to the as-built and to the specimen strengthened with the same material.

It is worth mentioning that the specimen strengthened with the fiberglass fabric (OOP_2E_EQ) exhibited a very slight damage during the test, with the formation of a noticeable crack (with no overturning of masonry parts or brick tiles) only in the very last part of the test, at the load-bearing capacity drop corresponding to conventional collapse. In addition, no visible damage was registered for the strengthening fabric.

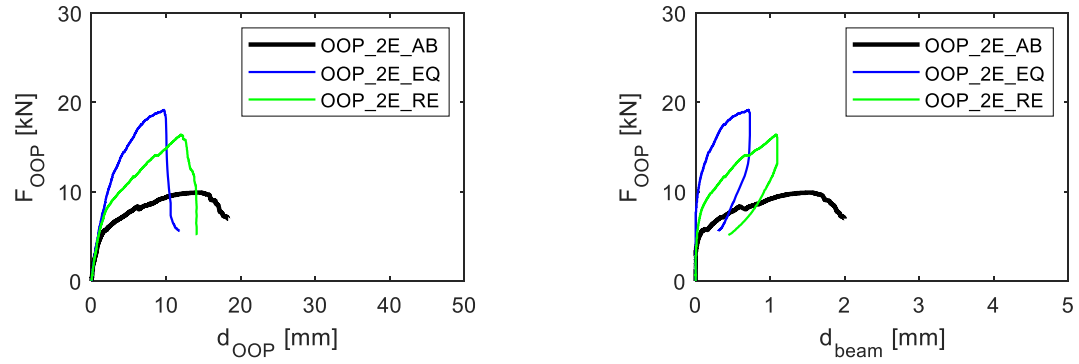

(a) (b)

Figure 16. Comparison of the responses of specimens: (a) OOP force-displacement, (b) OOP force-beam deflection.

specimen	strength [kN]	displacement at peak load [mm]	ultimate displacement [mm]	ductility
OOP_2E_AB	9.9	13.9	17.1	1.23
OOP_2E_EQ	19.1 (+93%)	9.7	10.1	1.04
OOP_2E_RE	16.3 (+65%)	12.1	13.0	1.07

Table 3. Comparison of significant tests' results for specimens OOP_2E_AB, OOP_2E_EQ, OOP_2E_RE.

5 CONCLUSIONS

In this study, out-of-plane experimental tests are performed on infill walls in RC frames. The results of four experimental tests are presented. The infill walls tested were: an as-built unreinforced masonry specimen (OOP_2E_AB), a specimen strengthened by applying an FRCM with fiberglass mesh (OOP_2E_RG), a specimen strengthened by applying a fiberglass fabric (OOP_2E_EQ). In addition, the as-built specimen was repaired after the first OOP test by applying the same fiberglass fabric adopted for specimen OOP_2E_EQ (specimen OOP_2E_RE).

The specimens were constructed to have only one-way vertical bending and/or one-way vertical arching action. The following significant conclusions can be drawn.

Specimen OOP_2E_AB exhibited an OOP strength equal to 9.9 kN; specimen OOP_2E_RG exhibited an OOP strength equal to 28.4 kN; specimen OOP_2E_EQ exhibited an OOP strength equal to 19.1 kN. The application of the FRCM

with fiberglass mesh increased the OOP strength by +187%; the application of the fiberglass fabric increased the OOP strength by +93%.

However, the strengthening techniques adopted did not influence the OOP ductility capacity of specimens. The repaired specimen exhibited an intermediate response with respect to specimens OOP_2E_AB and OOP_2E_EQ. More specifically, it exhibited a strength increment with respect to the as-built specimen roughly equal to 65%. It was observed, for all specimens, that the presence of a strengthening material delays the occurrence of arching action, i.e., increases the external load that the infill can withstand only with a flexural mechanism. Hence, the resistant mechanism of the one-way infills tested was ensured only by a flexural mechanism, first, then also by the presence of arching effect.

6 ACKNOWLEDGMENTS

This work was developed under the financial support of METROPOLIS (*Metodologie e tecnologie integrate e sostenibili per l'adattamento e la sicurezza di sistemi urbani - PON Ricerca e Competitività 2007-2013*) and *ReLUIS-DPC 2014-2018 Linea Cemento Armato – WP6 Tamponature*, funded by the Italian Department of Civil Protection (DPC). The reinforcing materials were provided by Mapei. These supports are gratefully acknowledged.

REFERENCES

Angel, R., Abrams, D.P., Shapiro, D., Uzarski, J., Webster, M., 1994. Behaviour of reinforced concrete frames with masonry infills. University of Illinois Engineering Experiment Station. College of Engineering. University of Illinois at Urbana-Champaign.

Binici, B., Ozcebe, G., Ozcelik, R., 2007. Analysis and design of FRP composites for seismic retrofit of infill walls in reinforced concrete frames. *Composites: Part B*, **38**, 575-583.

Calvi, G.M., Bolognini., D., 2001. Seismic response of reinforced concrete frames infilled with weakly reinforced masonry panels, *Journal of Earthquake Engineering*, **5**(2), 153-185.

D'Antino, T., Carozzi, F.G., Colombi, P., Poggi, C., 2018. Out-of-plane maximum resisting bending moment of masonry walls strengthened with FRCM composites, *Composite Structures*, **202**, 881-896.

da Porto, F., Guidi, G., Verlato, N., Modena, C., 2015. Effectiveness of plasters and textile reinforced mortars for strengthening clay masonry infill walls subjected to combined in-plane/out-of-plane actions. *Mauerwerk European Journal of Masonry*, **19**(5), 334-354.

Dawe, J.L., Seah, C.K., 1989. Out-of-plane resistance of concrete masonry infilled panels, *Canadian Journal of Civil Engineering*, **16**(6), 854–864.

Di Domenico, M., Ricci, P., Verderame, G.M., 2018. Experimental assessment of the influence of boundary conditions on the out-of-plane response of unreinforced masonry infill walls, *Journal of Earthquake Engineering*. (in press)

Di Domenico, M., Ricci, P., Verderame, G.M., 2019. Experimental assessment of the out-of-plane strength of URM infill walls with different slenderness and boundary conditions, *Bulletin of Earthquake Engineering*. (in press)

Furtado, A., Rodrigues, H., Arêde, A., Varum, H., 2016. Experimental evaluation of out-of-plane capacity of masonry infill walls, *Engineering Structures*, **111**, 48-63.

Guidi, G., da Porto, F., Dalla Benetta, M., Verlato, N., Modena, C., 2013. Comportamento sperimentale nel piano e fuori piano di tamponamenti in muratura armata e rinforzata. *15° Convegno ANIDIS L'Ingegneria Sismica in Italia*, June 30 – July 4, Padua, Italy. (in Italian).

Hrynyk, T.D., Myers, J.J., 2008. Out-of-plane behavior of URM arching walls with modern blast retrofits: experimental results and analytical model, *Journal of Structural Engineering*, **134**(10), 1589-1597.

Ismail, N., El-Maaddawy, T., Khattak, N., Walsh, K.Q., Ingham, J.M., 2018. Out-of-plane behaviour of in-plane damaged masonry infills strengthened using fibre reinforced matrix. *10th International Masonry Conference*, July 9-11, Milan, Italy.

Koutas, L.N., Bournas, D.A., 2019. Out-of-plane strengthening of masonry-infilled RC frames with textile-reinforced mortar jackets, *Journal of Composites for Construction*, **23**(1).

Longo, F., Wiebe, L., da Porto, F., Modena, C., 2018. Application of an in-plane/out-of-plane interaction model for URM infill walls to dynamic seismic analysis of RC frame buildings. *Bulletin of Earthquake Engineering*, **16**(12), 6163-6190.

Lourenço, P.B., Leite, J.M., Paulo-Pereira, M.F., Campos-Costa, A., Candeias, P.X., Mendes, N., 2016. Shaking table testing for masonry infill walls: unreinforced versus reinforced solutions, *Earthquake Engineering and Structural Dynamics*, **45**(14), 2241-2260.

Lunn, D.S., Rizkalla, S.H., 2011. Strengthening of infill masonry walls with FRP materials, *Journal of Composites for Construction*, **15**(2), 206-214.

Lunn, D.S., Rizkalla, S.H., 2014. Design of FRP-strengthened infill-masonry walls subjected to out-of-plane loading, *Journal of Composites for Construction*, **18**(3).

Mosalam, K.M., Günay, S., 2015. Progressive collapse analysis of reinforced concrete frames with unreinforced masonry infill walls considering in-plane/out-of-plane interaction, *Earthquake Spectra*, **31**(2), 921-943.

NTC2008, 2008. Decreto ministeriale 14 gennaio 2008 - Norme Tecniche per le Costruzioni. Supplemento ordinario n. 30 Gazzetta Ufficiale 4 febbraio 2008, n 29. (in Italian).

Pereira, M.F.P., Pereira, M.F.N., Ferreira, J.E.D., Lourenço, P.B., 2011. Behavior of masonry infill panels in RC frames subjected to in plane and out of plane loads. *7th international conference AMM 2001*, June 13-15, Krakow, Poland.

Ricci, P., Di Domenico, M., Verderame, G.M., 2018a. Empirical-based out-of-plane URM infill wall model accounting for the interaction with in-plane demand, *Earthquake Engineering and Structural Dynamics*, **47**(3), 802-827.

Ricci, P., Di Domenico, M., Verderame, G.M., 2018b. Experimental assessment of the in-plane/out-of-plane interaction in unreinforced masonry infill walls,

Engineering Structures, **173**, 960-978, 2018. doi: 10.1016/j.engstruct.2018.07.033.

Ricci, P., Di Domenico, M., Verderame, G.M., 2018c. Experimental investigation of the influence of slenderness ratio and of the in-plane/out-of-plane interaction on the out-of-plane strength of URM infill walls. *Construction and Building Materials*, **191**, 505-522.

Valluzzi, M.R., da Porto, F., Garbin, E., Panizza, M., 2014. Out-of-plane bending behavior of infill masonry panels strengthened with composite materials, *Materials and Structures*, **47**, 2131-2145.

Velazquez-Dimas, J.I., Ehsani, M.R., 2000. Modeling out-of-plane behavior of URM walls retrofitted with fiber composites, *Journal of Composites for Construction*, **4**(4), 172-181.

Verderame, G.M., Ricci, P., Di Domenico, M., 2019. Experimental vs. theoretical out-of-plane seismic response of URM infill walls in RC frames, *Structural Engineering and Mechanics*, **69**(6), 677-691.